Journal of Plankton Research Vol.17 no.2 pp.405–412, 1995

One-dimensional numerical simulation of primary production: Lagrangian and Eulerian formulations

Dennis J.McGillicuddy,Jr[1]

Department of Earth and Planetary Sciences, Harvard University, Cambridge, MA 02138, USA

[1]*Present address: Woods Hole Oceanographic Institution, Woods Hole, MA 02543, USA*

Abstract. It has been argued (Wolf and Woods, in *Toward a Theory On Biological–Physical Interactions in the World Ocean*, Rothschild, (ed.), 1988) (WW88) that phytoplankton growth models are sensitive to Lagrangian effects because populations at a given depth and time contain a wide distribution of photoadaptive properties. On the other hand, Lande and Lewis (*Deep-Sea Research*, **36**, 1161–1175, 1989) (LL89) have claimed that for a different photosynthetic model, this distribution of properties can be adequately represented by a mean value in a much simpler and more efficient Eulerian formulation. This study compares Lagrangian and Eulerian integrations of these two different models of photosynthesis under two mixing regimes. For relatively weak mixing, the growth rate predicted by the different formulations of the two models is small (≤5%). In vigorously mixed conditions, Lagrangian effects cause a significant (~20%) reduction in the mean growth rate of the WW88 model, while the differences in the two integrations of the LL89 model differ only slightly (~3%). The apparent discrepancy in the comparisons betwen Lagrangian and Eulerian integrations of the two different photosynthesis models is a result of different parameterizations of photoadaptive reaction kinetics.

Introduction

Two different approaches have been used to implement models of phytoplankton production in one-dimensional models of upper ocean physics. Eulerian formulations treat phytoplankton populations in terms of their bulk properties, and the aggregate photosynthetic response is computed at fixed grid points in the water column. Alternatively, Lagrangian formulations compute phytoplankton growth along the trajectories of individual fluid parcels. In this approach, a large number of particles must be modeled in order to resolve the profile of primary production with statistical significance. Woods and Onken (1982) were the first to introduce the use of the Lagrangian ensemble method for simulating upper ocean phytoplankton populations. From a theoretical point of view, the most important difference between these two approaches arises from the fact that phytoplankton continually adapt to a rapidly fluctuating light environment as they move vertically in the water column. The population at a given depth therefore has a distribution of photoadaptive properties that reflects the histories of the various individuals. Such a distribution of properties is computed explicitly in an ensemble of Lagrangian particles, while the classical Eulerian model represents this distribution with its mean. Clearly, the relationship between the photoadaptive response and the rate of mixing will determine whether or not the mean value of photoadaptive properties is sufficient to obtain accurate photosynthetic profiles.

Wolf and Woods (1988) (hereafter WW88) have stated that population growth

is sensitive to the 'diversity in the state of adaptation of a crowd of plankters that happen at any instant to occupy the same depth', and that their Lagrangian ensemble method is the most convenient way to represent this aspect of the population dynamics. Conversely, investigations by other authors (Falkowski and Wirick, 1985; Lande and Lewis, 1989) have documented much less sensitivity to Lagrangian effects in their models of photosynthesis and photoadaptation. In particular, Lande and Lewis (hereafter LL89) show in a carefully constructed analytic treatment of the problem that for relatively low mixing rates and reaction kinetics consistent with experimental data on *Thalassiosira pseudonana*, Lagrangian effects result in differences of <1% in photosynthetic rate. This paper seeks to reconcile this apparent controversy by comparing Lagrangian and Eulerian integrations of the two different photosynthesis models of WW88 and LL89 in idealized one-dimensional simulations in which the mixed layer depth is held constant and the solar forcing varies in a diel cycle.

Method

The biological models

In the WW88 model, the complex physiology of phytoplankton growth is reduced to its most fundamental requirements for energy in the form of light and nutrients (nitrate in this case). The model cell has two reservoirs in which it accumulates light and nutrients. When both cellular pools reach specified threshold values, the cell divides and its energy and nutrient reserves are distributed equally to both daughter cells. Both pools have maximum values at which the cells cease to accumulate reserves. This prevents the cells from unrealistic build-up of the non-limiting constituent. The threshold and maximum values, along with all other model parameters, are listed in Table I.

Phytoplankton cells capture inorganic nutrient through an active transport mechanism that can be characterized by Michaelis–Menten kinetics. Expressed mathematically, the instantaneous rate of short-term uptake, V (units of time^{-1}), is a hyperbolic function of substrate concentration, S (units of mass $\times$ volume^{-1}):

Table I. WW88 biological model parameters

Parameter	Value	Description
A_{cell}	$\pi \times 10^{-8}$ m^2	cellular cross-sectional area
V_{max}	1.0×10^{-3} μm NO_3 cell^{-1} h^{-1}	maximum rate of nutrient uptake
K_s	0.2 μm NO_3 l^{-1}	half-saturation constant for nutrient uptake
E_{resp}	2.0×10^{-7} J h^{-1}	cellular respiration rate
E_{thresh}	1.4×10^{-4} J	energy threshold for cell division
E_{max}	2.7×10^{-4} J	maximum cellular energy content
N_{thresh}	2.0×10^{-8} μm NO_3	nutrient threshold for cell division
N_{max}	3.8×10^{-8} μm NO_3	maximum cellular nutrient content
τ_P	5 h	photoadaptation time constant
F_1	0.3	photoadaptation factor

$$V = V_{max} \frac{S}{K_s + S} \quad (1)$$

The two parameters V_{max} and K_s determine the shape of the hyperbola by specifying the asymptotic uptake value at high substrate concentrations and the steepness of the curve at lower values, respectively. In these simulations, a very high value for V_{max} has been used so that nutrient uptake is essentially instantaneous and the dynamics of a purely light-limited population can be investigated.

The energy absorbed by each cell, E_{abs}, depends both on the amount of light incident upon its effective cross-sectional area, A_{cell}, and a photoadaptive efficiency factor, P_E:

$$E_{abs} = I(z,t) \times A_{cell} \times P_E \quad (2)$$

The efficiency factor is given by:

$$P_E = F_1 \times \exp\left(\frac{-I(z,t)}{I_m}\right); \qquad I_m = \frac{1}{\tau_P} \int_{t-\tau_P}^{t} I(z,t)dt \quad (3)$$

where F_1 is a constant and I_m is the mean irradiance that the cell has been exposed to over the photoadaptation period τ_P. The phytoplankton cells suffer a constant respiratory loss from their energy pool of 2.0×10^{-7} J h^{-1}.

The LL89 model predicts the rate of photosynthesis, P, as a function of the ambient light intensity using:

$$P(I;\alpha,P_s,\beta) = P_s(1 - e^{(-\alpha I/P_s)})\, e^{(-\beta I/P_s)}$$

The photosynthetic parameters α, P_s and β are each assumed to have fully adapted values Γ_i^* which are linear functions of the logarithm of the light intensity:

$$\Gamma_i^* = c_i + m_i \ln I$$

and that the populations adapt their instantaneous values Γ_i to the fully adapted state according to first-order reaction kinetics:

$$\frac{\partial \Gamma_i}{\partial t} = \gamma_i (\Gamma_i^* - \Gamma_i)$$

Table II lists the parameter values used in the LL89 photosynthetic model.

Implementation of the biological models in Lagrangian and Eulerian frameworks

The difference between the Eulerian and Lagrangian formulations lies in the treatment of cell trajectories. In the Lagrangian formulation, particles in the mixing layer are assumed to be randomly distributed on a time scale

Table II. LL89 photosynthetic model parameters

Photosynthetic trait	γ_i (h^{-1})	c_i	m_i
α (μg C μg Chl^{-1} h^{-1} (μE m^{-2} s^{-1})$^{-1}$)	0.58	0.0527	−0.00468
P_s (μg C μg Chl^{-1} h^{-1})	0.29	−0.860	0.968
β (μg C μg Chl^{-1} h^{-1} (μE m^{-2} s^{-1})$^{-1}$)	0.5	0.00438	-7.33×10^{-4}

characteristic of the turnover of the mixing layer. Assuming that the local rate of supply of turbulent kinetic energy is in approximate balance with the rate of dissipation, ϵ, the relationship between the velocity scale u and length scale l of the large eddies and the viscous dissipation at the Kolmogorov microscale is (Taylor, 1935; Tennekes and Lumley, 1972; Gargett, 1988):

$$\epsilon \sim \frac{u^3}{l} \tag{4}$$

Given that the vertical extent of the largest eddies in the mixing layer is set by the depth of the mixing layer, a characteristic turbulent velocity can therefore be calculated from an estimate of the rate of dissipation. The turnover time of the mixing layer, τ_m, is thus given by $\tau_m = (l/u)$. The Lagrangian trajectories of the model cells are computed assuming that the particles in the mixing layer are uniformly distributed on this time scale, i.e. a new turbulent velocity between $-(u/2)$ and $(u/2)$ is randomly chosen for each particle in the mixing layer after every turnover time. Thus, the velocity of individual particles changes once every $(\tau_m/\Delta t)$ time steps. In situations when the number of particles in a 1 m depth interval falls below 20 (a number chosen to maintain statistical significance), each particle in that interval is divided into two particles with half the biomass. WW88 introduced this technique to ensure adequate resolution of the simulated biological and chemical profiles. In the present model, cell sinking is not considered so there is no flux of biomass out of the mixed layer.

In the Eulerian formulation, the cell trajectories are not treated explicitly. Phytoplankton growth is calculated at a set of discrete depths (1 m apart) in the water column. The water properties ϕ (i.e. the phytoplankton biomass and the dissolved nutrient) are mixed using an eddy diffusion mixing parameterization:

$$\frac{\partial \phi}{\partial t} = K_z \frac{\partial^2 \phi}{\partial z^2}$$

subject to the boundary condition $(\partial\phi/\partial z) = 0$ at the surface and bottom of the mixed layer. The eddy diffusivity K_z scales with the characteristic velocity and length (Tennekes and Lumley, 1972):

$$K \sim ul$$

This scale relationship is not an exact equation. In practice, the proportionality constant must be obtained empirically. For the present purposes, this was

Table III. Physical model parameters

Parameter	Value	Description
k	0.04 m^{-1}	diffuse attenuation coefficient
K_z	0.01, 4.64 $m^2 s^{-1}$	eddy diffusion coefficient
Δz	1 m	vertical resolution
Δt	21.6, 0.1 s	time step

Table IV. Results of numerical simulations. The integration scheme in each run is denoted as either E (Eulerian) or L (Lagrangian). $\bar{P}$ is the mean daily growth rate, and the last column is the normalized difference between mean daily growth rates in the Lagrangian and Eulerian integrations

Run	Integration scheme	Photosynthesis model	K_z ($m^2 s^{-1}$)	$\bar{P}$ (day^{-1})	$\frac{\bar{P}_L - \bar{P}_E}{\bar{P}_E}$
1	E	LL89	0.01	1.1035	
2	L	LL89	0.01	1.0735	−2.7%
3	E	WW88	0.01	0.3454	
4	L	WW88	0.01	0.3273	−5.2%
5	E	LL89	4.64	1.0246	
6	L	LL89	4.64	1.0545	+2.9%
7	E	WW88	4.64	0.3542	
8	L	WW88	4.64	0.2813	−20.6%

accomplished by performing twin Lagrangian and Eulerian simulations in which photoadaptation was excluded from the WW88 biological model by assuming a constant photosynthetic efficiency factor P_E. Without photoadaptation, the predicted photosynthetic response should be identical in the two different formulations assuming that the mixing parameterizations are equivalent. The results of this experiment indicate that a proportionality constant of one does in fact result in eddy diffusion that is consistent with the Lagrangian mixing rates.

Results

The following numerical experiments document the differences between Lagrangian and Eulerian integrations of the two different models of photosynthesis described above. The physical model parameters are listed in Table III. The light environment $I(z,t)$ is simulated with a simple exponential extinction of a temporally varying surface intensity $I_0(t)$:

$$I(z,t) = I_0(t)e^{-kz} \tag{5}$$

where a truncated sinusoidal function is used for $I_0(t)$ to approximate the diel light fluctuations during the vernal equinox at 40°N. The initial conditions for the simulations are a uniform 5 μM nitrate profile and an even biomass distribution of 1.0×10^6 cells l^{-1} which is initially distributed into 50 particles in the Lagrangian simulations. The initial nutrient concentration is sufficient to preclude any nutrient limitation in the simulations with the WW88 model. The depth of the mixing layer is held constant at 100 m and the simulations are run

for a total of 10 days. Mean daily growth rates are computed from the last 5 days of each experiment to avoid the initial transient response as the models settle into regular repeating daily cycles.

A summary of the results is given in Table IV. Identical twin experiments were conducted in Lagrangian and Eulerian frameworks for both biological models in two different mixing regimes. In the first two twin experiments (runs 1–4), the relatively weak mixing rate used by LL89 ($K_z = 0.01$ m^2 s^{-1}) was applied. According to the scaling arguments described above, this corresponds to a mixed layer turnover time of 277 h. In the second set of twin experiments (runs 5–8), the eddy diffusion is much higher ($K_z = 4.64$ m^2 s^{-1}) in order to simulate the vigorous mixing of an actively convecting mixed layer. Again using the scaling arguments, this is consistent with a rate of dissipation of 1.7×10^{-6} W kg^{-1}, which is in agreement with measured values for mixing layers of similar vertical extent (Gargett *et al.*, 1979; Shay and Gregg, 1984). In this regime, the turnover time is ~30 min.

For relatively weak mixing (runs 1–4), the Lagrangian integrations of both biological models predict lower mean growth rates due to photoinhibition. Here it is important to note that regardless of the physical formulation the photosynthetic rates in the two biological models are quite different, with the LL89 model about a factor of three higher. It would be possible to tune the parameters of one or the other biological models in order to make their mean growth rates more comparable, but this has not been done. Instead, the differences between the Eulerian and Lagrangian integrations reported in Table IV are normalized by the Eulerian mean growth rate. Runs 1–4 show that the proportional differences between the Lagrangian and Eulerian integrations for the WW88 model are approximately a factor of two higher than for the LL89 model, but are still quite small (5.2%). The proportional difference in the simulations using the LL89 model is similar in magnitude to that reported by LL89, but slightly higher in the present study owing to the use of a diel light cycle rather than the constant surface light intensity.

In the strong mixing regime, the proportional difference in the two integrations of the LL89 model is still quite small (2.9%), but in the opposite sense as in the weak mixing case. The distribution of properties at each depth in the Lagrangian model serves to increase the average rate of photosynthesis as compared with the Eulerian formulation. The opposite is true for the WW88 biological model, in which photoinhibition plays the dominant role, decreasing the mean growth rate by nearly 21% in the Lagrangian integration.

Discussion

The preceding experiments demonstrate the sensitivities of two different biological models to the choice of physical formulation in idealized one-dimensional simulations under two mixing regimes. The LL89 photosynthesis model is rather insensitive to the physical formulation, as the proportional difference between Lagrangian and Eulerian integrations is <3% for both strong and weak mixing. The WW88 model is more sensitive to the physical

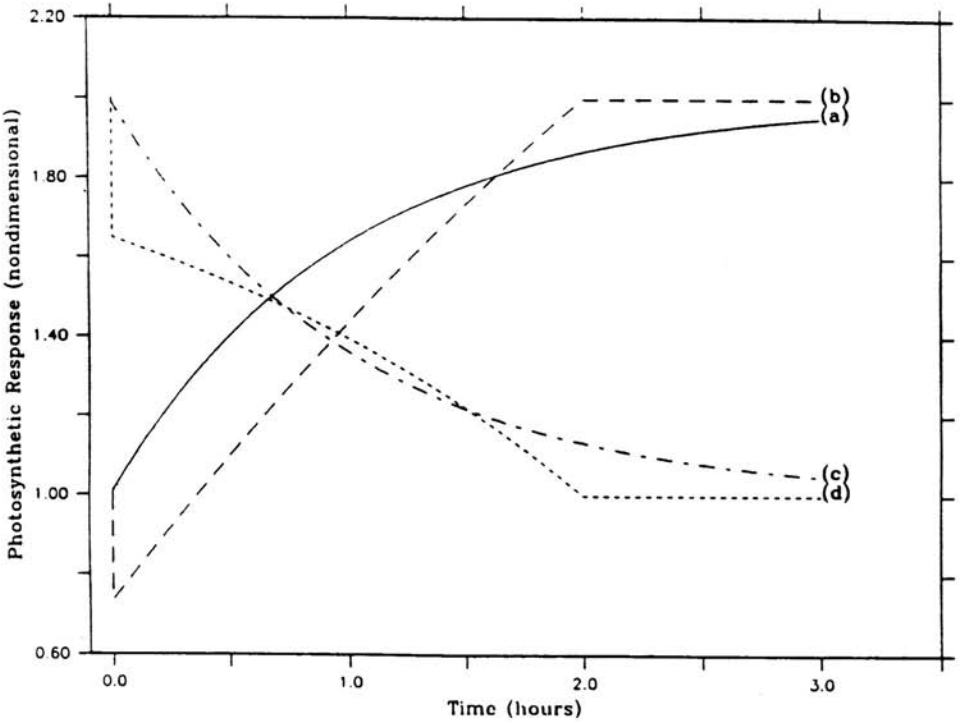

Fig. 1. Photosynthetic response to step functions in light intensity (see the text).

formulation, particularly in the strong mixing case in which photoinhibition significantly reduces the photosynthetic response.

The reason for the apparent discrepancy between the WW88 and LL89 models lies in the photoadaptive reaction kinetics. For comparison, the photosynthetic response of the two models to step functions in light intensity is shown in Figure 1. The first-order reaction kinetics used in LL89 produce an asymptotic response to an increase in light intensity [Figure 1, curve (a)]. The WW88 model's integral exponential kinetics cause the photosynthetic efficiency to fall immediately after the light is increased [Figure 1, curve (b)]. Although the fully adapted state is reached more quickly than in the case of first-order kinetics, the photosynthetic efficiency of this model is less during most of the adaptation period. Curves (c) and (d) in Figure 1 show the adjustment of the first-order and exponential models to lower light intensity. As in the previous case, the exponential kinetics cause an immediate decrease in photosynthetic efficiency [Figure 1, curve (d)]. Again, the fully adapted state is reached more quickly, but the early portion of the adaptation curve lies well below that of the first-order case. Thus, for both increases and decreases in light intensity, the integral exponential reaction kinetics cause the phytoplankton cells in this model to undergo significant immediate losses in photosynthetic efficiency. Given the fact that phytoplankton in the mixed layer are being mixed on a time scale much

shorter than the photoadaptive period, the cells in this model are always in the early portion of the photoadaptive curve. It is therefore clear why the WW88 model would tend to exaggerate the Lagrangian effects of photoadaptation—the reaction kinetics are such that the phytoplankton are in a continuous state of light shock. Thus, it appears that most of the discrepancy between the two models could be reconciled were both to use similar formulations of photoadaptation. In general, the literature appears more consistent with LL89's choice of first-order reaction kinetics (Falkowski, 1980, 1983, 1984; Marra, 1980; Rivkin *et al.*, 1982; Lewis *et al.*, 1984; Vincent *et al.*, 1984).

Acknowledgements

This work was carried out while the author was supported by an Office of Naval Research Graduate Fellowship and subsequently Office of Naval Research grant N00014-90-J-1593. The very helpful comments and suggestions offered by J.J.McCarthy, J.D.Woods, K.U.Wolf, A.K.Suri and A.R.Robinson are greatly appreciated.

References

Falkowski,P. (1980) Light–shade adaptation in marine phytoplankton. In Falkowski,P. (ed.), *Primary Productivity in the Sea.* Plenum Press, New York, 531 pp.

Falkowski,P. (1983) Light–shade adaptation and vertical mixing of marine phytoplankton: A comparative field study. *J. Mar. Res.*, **41**, 215–237.

Falkowski,P. (1984) Kinetics of adaptation to irradiance in *Dunaliella tertiolecta. Photosynthetica*, **18**, 62–68.

Falkowski,P. and Wirick,C.D. (1985) A simulation model of the effects of vertical mixing on primary productivity. *Mar. Biol.*, **65**, 69–75.

Gargett,A. (1988) A 'large-eddy' approach to acoustic remote sensing of turbulent kinetic energy dissipation rate ϵ. *Atmos.-Ocean*, **26**, 483–508.

Gargett,A., Sanford,T.B. and Osborn,T.R. (1979) Surface mixing layers in the Sargasso Sea. *J. Phys. Oceanogr.*, **9**, 1090–1111.

Lande,R. and Lewis,M.R. (1989) Models of photoadaptation and photosynthesis by algal cells in turbulent mixed layer. *Deep-Sea Res.*, **36**, 1161–1175.

Lewis,M., Cullen,J.J. and Platt,T. (1984) Relationships between vertical mixing and photoadaptation of phytoplankton: similarity criteria. *Mar. Ecol. Prog. Ser.*, **15**, 141–149.

Marra,J. (1980) Vertical mixing and primary production. In Falkowski,P. (ed.), *Primary Productivity in the Sea.* Plenum Press, New York, 531 pp.

Rivkin,R., Seliger,H.H., Swift,E. and Biggley,W.H. (1982) Light–shade adaptation by the oceanic dinoflagellates *Pyrocystis noctiluca* and *P.fusiformis. Mar. Biol.*, **68**, 181–191.

Shay,T. and Gregg,M.C. (1984) Turbulence in an oceanic convective mixed layer. *Nature*, **310**, 282–285.

Taylor,G. (1935) Statistical theory of turbulence. *Proc. R. Soc. London*, **151**, 421.

Tennekes,H. and Lumley,J.L. (1972) *A First Course in Turbulence.* MIT Press, Cambridge, MA, 300 pp.

Vincent,W., Neale,P.J. and Richerson,P.J. (1984) Photoinhibition: algal responses to bright light during diel stratification and mixing in a tropical alpine lake. *J. Phycol.*, **20**, 201–211.

Wolf,K. and Woods,J.D. (1988) Lagrangian simulation of primary production in the physical environment—the deep chlorophyll maximum and nutricline. In Rothschild,B. (ed.), *Toward a Theory on Biological–Physical Interactions in the World Ocean.* D.Reidel, Dordrecht.

Woods,J. and Onken,R. (1982) Diurnal variation and primary production in the ocean—preliminary results of a Lagrangian ensemble model. *J. Plankton Res.*, **4**, 735–756.

Received on December 26, 1993; accepted on October 2, 1994